Journal of Materials Chemistry B

Accepted Manuscript

ROYAL SOCIETY OF CHEMISTRY

www.rsc.org/materialsB

Modulation of protein adsorption, vascular cell selectivity and platelet adhesion by mussel-inspired surface functionalization

Yonghui Ding[a], Zhilu Yang[b], Cathy WC Bi[c], Meng Yang[a], Jingcheng Zhang[a], Sherry Li Xu[c], Xiong Lu[b], Nan Huang[b], Pingbo Huang[c,d, and e], Yang Leng[a*]

[a]*Department of Mechanical and Aerospace Engineering, The Hong Kong University of Science and Technology, Clear Water Bay, Kowloon, Hong Kong*
Email: meleng@ust.hk

[b]*Key laboratory of Advanced Technology of Materials, School of Material Science and Engineering, Southwest Jiaotong University, Chengdu, 610031, Sichuan, China*

[c]*Division of Life Science, The Hong Kong University of Science and Technology, Clear Water Bay, Kowloon, Hong Kong*

[d]*Division of Biomedical Engineering, and* [5]*State Key Laboratory of Molecular Neuroscience, The Hong Kong University of Science and Technology, Clear Water Bay, Kowloon, Hong Kong*

Abstract

A mussel-inspired surface functionalization of polydopamine (PDA) coating has been demonstrated to be a promising strategy to ensure the biocompatibility of various biomaterials. To explore the multifunctionality of the PDA coating for vascular stents and elucidate the mechanisms by which the PDA coating modulates vascular cell behavior, this study examined the protein adsorption, the responses of endothelial cells (ECs) and smooth muscle cells (SMCs), and platelet adhesion to various PDA-coated surfaces synthesized at varied initial dopamine concentrations. Our results indicate that various PDA coatings present distinct and varied functionalities. The quinone group on the PDA coating induces a substantially higher amount of protein adsorption, which subsequently plays a key role in promoting EC attachment and proliferation by regulating their focal adhesion and stress fiber formation. Meanwhile, the reactive phenolic hydroxyl group on the PDA coating potently inhibits SMC proliferation. In addition, the quinone-regulated fibrinogen adsorption to the PDA coating may increase platelet adhesion. Notably, the PDA coating synthesized at initial dopamine concentration of 1.0 g/L shows the most favorable vascular cell selectivity. These findings shed light on the relationships between surface characteristics, protein adsorption, vascular cell behavior, and platelet adhesion of the PDA coating, which may guide better design of PDA application in vascular stents.

Keywords: *polydopamine, surface property, protein adsorption, vascular cell selectivity, platelet adhesion*

1. Introduction

Cardiovascular diseases that usually result from malfunction in coronary arteries remain the leading cause of morbidity and mortality worldwide. Vascular prosthetics such as stents are commonly used in the treatment for these diseases. However, such implantations are associated with major complications such as in-stent restenosis caused by the proliferation of vascular smooth muscle cells (SMCs) and late-stent thrombosis induced by inadequate re-endothelialization on the surface and poor hemocompatibility of the vascular stents. Thus, an ideal stent should favor re-endothelialization while concomitantly inhibiting smooth muscle cell (SMC) proliferation and improving hemocompatibility.

Polydopamine (PDA) has attracted considerable interest because it provides not only facile functionalization of various substrates but also good biocompatibility. However, previous studies have provided limited or even debatable information about the mechanism by which the PDA coating modulates cell behavior. It has been suggested that favorable adsorption of serum protein with preserved bioactivity was the main contributor to enhanced cell adhesion on the PDA-coated surfaces [1-4]. Wu et al. also indicated that improved apatite mineralization, and subsequently benefited protein adsorption contributed to enhanced proliferation and differentiation of the cells [7-9]. However, Yang et al. [5] and Luo et al. [6] observed inhibitory effects on smooth muscle cell (SMC) proliferation induced by the PDA-coated surface and argued that phenolic/quinone groups presented on the PDA coating other than adsorbed serum

protein layer played a key role in modulating vascular cell behavior. It is well described that surface properties determine the protein adsorption profile, i.e. the composition, amount and conformation of adsorbed proteins [10], and mediate the subsequent cell responses such as platelet adhesion, and vascular cell attachment and growth [11-13]. Therefore, to understand the mechanism by which the PDA coating modulates vascular cell behavior, the inherently correlated three aspects, "surface property – protein adsorption – vascular cell behavior", must be systematically studied.

Recently, it was reported that the PDA coatings synthesized under different sets of conditions, including coating time, temperature, initial dopamine concentrations, pH of solution, and oxidants employed, can give rise to physically and chemically different surface property [14-16]. However, little is known about the influence of the varying synthetic conditions of the PDA coating on the cellular responses, except the findings of several-minutes PDA deposition being sufficient to induce significantly enhanced cell adhesion [4, 17]. Herein, we hypothesized that varying physicochemical properties of PDAs synthesized under varied conditions might help elucidate the complex interactions among surface property, protein adsorption and vascular cell behavior.

In this study, we examine physicochemical properties of the PDA coatings synthesized at various initial dopamine concentrations, and investigate its influence on relevant protein adsorptions, vascular cell and platelet behavior. By performing this type of systematic study, we propose a mechanism of PDA modulating vascular

cell behavior, which may provide rational strategy directed at tailoring functionality of PDA.

2. Materials and experiments

2.1 Preparation of the PDA coating

The PDA coatings were made on TiO_2 substrates that was prepared by sputtering Ti on silicon wafer with post-heat treatment to obtain well-controlled TiO_2 substrate finishing and properties as previously described [18]. The TiO_2 substrates for PDA coatings were immersed into dopamine solutions with various initial dopamine concentrations (0.25, 0.5, 1.0, 2.0, 4.0 g/L in 10 mM Tris buffer, pH 8.5) at 25 ℃ for 12 h in an open vessel. After that, the PDA-coated substrates were vigorously washed with DI water and blown dry under a slight stream of nitrogen. For the use of cell culture, the specimens were further sterilized with 73% ethanol in Milli-Q water for 30 min just before being used.

2.2 Characterization of the PDA coating

The surface elemental compositions were examined by X-ray photoelectron spectroscopy (XPS; Kratos, Axis Ultra DLD). An X-ray monochromatic Al K-α was used as excitation source (hν = 1486.6ev) running at 15kV and 150 W. Atomic percentages of the various elements were derived from broad range spectra, using the Al source in a low-resolution mode (pass energy 160 eV), while a pass energy of 20 eV was used for high-resolution spectra of the Ti 2p, C 1s, N 1s, and O 1s. The C 1s

peak (binding energy 285.0 eV) was used as a reference for charge correction. In addition, the quantification of the relative amount of reactive phenolic hydroxyl groups presented on the PDA coating was performed with a Micro-BCA assay [19]. In brief, the specimens were immersed in 300 μl Micro-BCA working solution (Pierce, IL, USA) and incubated at 37 ℃ for 120 min. The working solution that reacted with reactive phenolic hydroxyl groups on the PDA coating was detected at 562 nm using a microplate reader.

Surface wettability of the PDA coating was examined by water contact angle (WCA) measurements with a contact angle instrument (Digidrop, France) and applying the sessile drop method. The zeta potentials of the various surfaces were examined with a commercial electro kinetic analyzer (EKA, Anton Paar GmbH, Graz, Austria). For each specimen, zeta-potential was measured in a solution of 0.001 M KCl (pH = 7.4) at room temperature.

2.3 Protein adsorption

Single protein solutions of bovine serum albumin (300 μg/ml, Sigma-Aldrich, USA), human fibrinogen (300 μg/ml, Sigma-Aldrich, USA), and human fibronectin (100 μg/ml, Sigma-Aldrich, USA) were prepared in phosphate buffered saline (PBS, pH = 7.4). Complex protein solution was prepared by Dulbecco's Modified Eagle Medium: Nutrient Mixture F-12 (DMEM/F12) culture medium supplemented with 10% fetal bovine serum (FBS). The zeta-potentials of prepared protein solutions were determined with a Zeta Potential Analyzer from Brookhaven Instruments Corporation.

Quantification of protein adsorptions was carried out at room temperature using a quartz crystal microbalance equipped with dissipation monitoring (QCM-D, Q-sense AB, Sweden). Prior to the measurement, the PDA coating was deposited on an AT-cut 5 MHz Au coated quartz crystal (diameter of Au films: 10 mm) at various initial dopamine concentrations. Initially, the PDA-coated quartz crystal was mounted in the QCM chamber and PBS solution (pH = 7.4) was injected at 50 μL/min continuously until the QCM trace stabilized. After that, the prepared protein solution was passed through the measuring chamber in contact with the crystal at the same speed, ultimately rinsed with PBS solution (pH = 7.4). The measured frequency shift (Δf) was converted into the adsorbed mass change (Δm) according to the Sauerbrey relation [20].

2.4 Vascular cell culture

Human umbilical vein endothelial cells (HUVECs) were cultured in 0.2%-gelatin-coated T75 flasks with Lonza Endothelial Growth Medium (EGM) bullet kit containing 100 U/ml penicillin and 100 U/ml streptomycin in a humidified incubator with 95% air and 5% CO_2. HUVECs between passages 2 and 7 were used for experiments to ensure the genetic stability of the cultures. HUVECs were plated on the specimens at a density of 7,500 cells/cm^2 and incubated for various periods (2, 24, and 72 h).

Human umbilical artery smooth muscle cells (HUASMCs) were obtained through the slow outgrowth of the cells from small pieces of umbilical artery in media,

and were cultured in DMEM/F12 medium containing 10% fetal bovine serum. The culture medium was changed every 3 days. The cells were subcultured when they were larger than 80% confluent and the cells were used in experiments between passages 2 and 5. HUASMCs were plated on the specimens at a density of 5×10^4 cells/cm^2 and incubated for the same periods as the HUVECs.

2.5 HUVEC attachment, proliferation, morphology and focal adhesion analysis

Cell attachment and proliferation were evaluated based on cell number on the surfaces after 2, 24, and 72 h in culture. To perform these evaluations, HUVECs cultured on the specimens were fixed with 4% paraformaldehyde (PFA; Sigma-Aldrich, USA) in phosphate buffered saline (PBS) for 20 min at room temperature. The cells were then permeabilized using 0.5% Triton X-100 in PBS for 5 min and blocked with 1% bovine serum albumin (BSA; Sigma-Aldrich) in PBS for 60 min to reduce nonspecific staining. Subsequently, to examine cytoskeletal formation, the cells were labeled for F-actin by using phalloidin conjugated to tetramethyl rhodamine isothiocyanate (TRITC) (2 μg/mL; Sigma-Aldrich) for 60 min at room temperature. The cells were also counter-stained with DAPI (1 μg/mL; Sigma-Aldrich) to observe the nuclei. To examine the focal adhesions in HUVECs, the cells were first stained with monoclonal anti-human vinculin antibodies (no. ab18058, 1:50 dilution; Abcam, Cambridge, UK) overnight at 4 ℃. After washing with PBS, the cells were incubated for 60 min with goat polyclonal secondary antibodies against mouse IgG (H&L, FITC-linked; no. ab6785, 1:500 dilution; Abcam). The specimens were finally washed three times in

PBS and mounted on microscope slides for examination using confocal laser scanning microscopy (LSM710, Zeiss, Germany). For quantitation, images were collected using 20×, 40×, and 63× objectives. The number and morphology of both cells and FAs were analyzed using ImageJ software (NIH, USA).

2.6 Determination of HUVEC phenotype

We used immunostaining to analyze the expression of two key endothelial cell markers: platelet endothelial cell adhesion molecule (PECAM-1/CD31) and von Willebrand factor (vWF). HUVECs were plated on the specimens at a density of 25,000 cells/cm^2. After incubation for 24 h, the cells were fixed with 4% PFA in PBS, permeabilized using 0.5% Triton X-100, blocked with 1% BSA, treated with primary antibodies overnight at 4 ℃, incubated with secondary antibodies for 60 min at room temperature, and finally counter-stained with DAPI. Antibodies were used at the following dilutions: 1:20 for monoclonal mouse anti-human CD31 antibody (Dako, Copenhagen, Denmark), 1:200 for polyclonal rabbit anti-human vWF antibody (Dako), and 1:500 for FITC-linked goat polyclonal secondary antibodies against mouse IgG.

2.7 HUASMC identification and proliferation

HUASMCs were identified by immunostaining with rat anti-human α-smooth muscle actin (α-SMA) primary antibodies and FITC-labeled sheep-anti-rat IgG. HUASMC proliferation was investigated by Cell Counting Kit-8 (CCK-8, Dojindo Laboratories)

after incubation for 24 and 72 h, respectively. The medium was removed and the specimens were washed once with PBS. Subsequently, 350 μl fresh DMEM-F12 medium containing 10% CCK-8 reagent was added to each specimen and incubated at 37 ^{o}C for 3 h in standard culture conditions. Afterward, each 200 μl of these solutions was transferred to a 96-well plate. The absorbance was measured at 450 nm by a microplate reader.

2.8 Platelet adhesion

The protocol used to evaluate platelet adhesion has been described in our previous report [18]. Briefly, to prepare platelet-rich plasma (PRP), whole blood was centrifuged (200 × *g*, 15 min) and the supernatant was collected. The PRP (50 μl) was placed on the surface of specimens and incubated at 37 ℃ for 2 h. After washing in PBS, the specimens with adherent platelets were fixed with 2.5% glutaraldehyde for 1 h at room temperature. The specimens were rinsed three times with PBS and then dehydrated using an ethanol series (30%, 50%, 75%, 90%, and 100%; 15–30 min each), and subsequently maintained in 100% ethyl alcohol until drying. After critical point drying, the specimens were mounted on copper stubs and sputter-coated with gold for examination by scanning electron microscopy (SEM, JSM-6390, JEOL, Japan).

2.9 Statistical analysis

All data are expressed as mean ± standard deviation (s.d.). All the cell data were quantified from at least 3 independent experiments, each with at least 3 replicates. Statistical analysis was performed using one-way analysis of variance (ANOVA), and $p \leq 0.05$ was considered statistically significant.

3. Results

3.1 Physicochemical properties

3.1.1 Chemical components

The PDA-coated specimens synthesized at different dopamine concentrations, 0.25 – 4 g/L, were named as 0.25PDA, 0.5PDA, 1.0PDA, 2.0PDA, and 4.0PDA for convenience. XPS wide spectra suggested the successful deposition of PDA on the substrate (Figure 1A). Ti and O are main elements detected in the pristine TiO_2 surface. After PDA coating, the peak intensity of C 1s and N 1s significantly increased, while the peak intensity of Ti 2p3 dramatically reduced or almost vanished. Moreover, through devolution high-resolution spectra of C 1s, O 1s and N 1s (Figure S1), it was demonstrated that the PDA coating contained three major functional groups, i.e. phenolic hydroxyl, quinone, and primary amino, which are consistent with literature [5, 6]. However, there were no significant differences in the percentage of these three functional groups on the various PDA coatings.

It is known that not only the number but also the positioning and arrangement of phenolic hydroxyl groups influence the antioxidant activity of polyphenol [21]. The micro-BCA assay revealed the amount of reactive phenolic hydroxyl groups, i.e. –OH

groups with antioxidant activity, presented on the various PDA coatings (Figure 1B). Note that the reaction of the micro-BCA assay relies on the reduction of cupric ion (Cu^{2+}) to cuprous ion (Cu^{1+}) by proteins, which can be achieved only by the reactive phenolic hydroxyl group on the PDA coatings. Interestingly, the amount of reactive phenolic hydroxyl groups displayed biphasic dependence on initial dopamine concentrations: it increased with concentrations initially but declined when the concentration reached above 1.0 g/L.

3.1.2 Physical properties

The surface wettability and surface charge are considered to be two main physical factors involved in protein adsorption and cell responses. The water contact angle (WCA) measurement showed that the PDA coating slightly increased surface hydrophobicity with respect to the pristine TiO_2 substrates, and all WCA values of PDAs were around 56 – 70^o (Figures 1C and S2). The surface charge (zeta potential) measurement showed that all surfaces were negatively charged at pH 7.4 (Figure 1D). All the PDA coatings displayed more negative charges compared to the pristine TiO2 surface, but there was no significant difference among them.

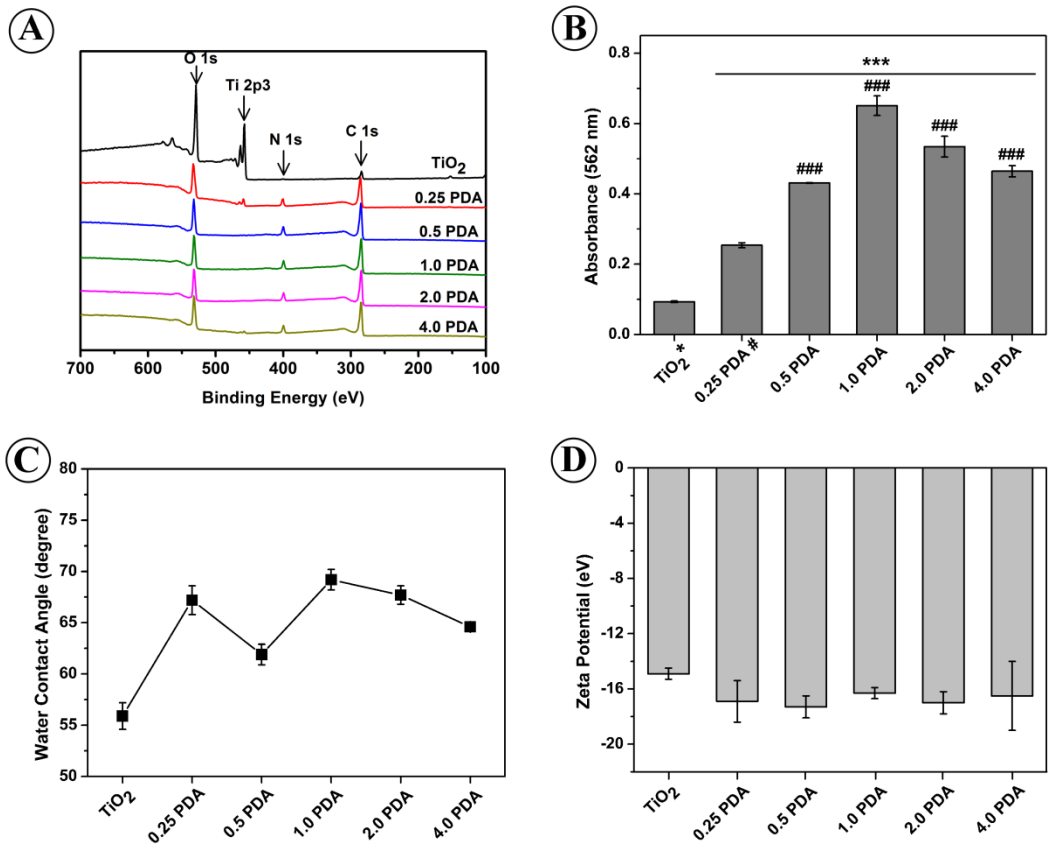

Figure 1. Physicochemical properties of the PDA and TiO_2 surfaces. (A) XPS wide spectra, (B) reactive phenolic hydroxyl groups determined via micro-BCA assay, (C) water contact angles (WCAs), and (D) zeta potentials. Statistically significant differences are marked as follows: * vs. TiO2; # vs. 0.25PDA .

3.2 Protein adsorption

Figure 2 revealed that the amount of both single protein adsorption and total protein adsorption to the PDA coatings was substantially higher than that to TiO_2 (see Figure S3 for mass shift vs. time curves). Significant differences in protein adsorption were also observed on the various PDA coatings. The bovine serum albumin (BSA) adsorption to 0.25PDA was at least 2-fold higher than that to other PDA coatings, 10

μg/cm^2 on 0.25PDA comparing with 3.8 μg/cm^2 on 0.5PDA and 5.1 μg/cm^2 on 1.0PDA. The fibrinogen (Fg) adsorption to 0.25PDA also showed the highest level of 15.6 μg/cm^2 among all the PDA coatings, while the relatively low levels of approximately 12.7 μg/cm^2 were observed on 1.0PDA and 2.0PDA. The fibronectin (Fn) adsorption to 0.25PDA, 0.5PDA and 1.0PDA was comparable and higher than that to other surfaces. TiO_2 and 2.0PDA displayed similar Fn adsorption levels, which were much lower than those to other surfaces. In addition, regarding to total protein adsorption from fetal bovine serum (FBS), 1.0PDA showed significantly higher levels, while 2.0PDA and 4.0PDA showed the lowest levels among the various PDA coatings.

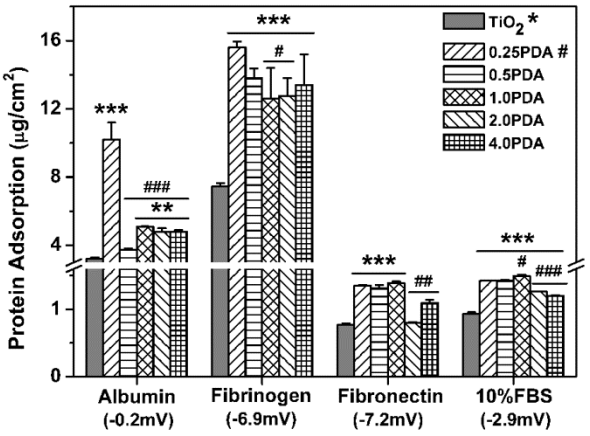

Figure 2. Quantitative comparison of protein adsorption to the PDA and TiO_2 surfaces: bovine serum albumin (BSA), fibrinogen (Fg), fibronectin (Fn), and 10% fetal bovine serum (FBS) in DMEM/F12 medium. Statistically significant differences are marked as follows: * vs. TiO2; # vs. 0.25PDA.

3.3 HUVEC responses

3.3.1 Attachment, proliferation, and morphology

HUVECs exhibited good attachment, spreading, and proliferation on all surfaces tested (Figure 3A). The quantitative data in Figure 3B revealed that the cell attachment number on the PDA coatings was larger than TiO_2 after 2 h culturing. Various PDA coatings showed different numbers of cell attachment: 0.5PDA, 1.0PDA and 2.0PDA showed significantly higher cell attachment number than 4.0PDA. After 24 and 72 h culture, the cell density on various surfaces displayed a similar trend to the cell attachment at 2 h: the cell density on all the PDA coatings was substantially higher than that on TiO_2, and 4.0PDA showed much lower cell density than other PDA coatings. This trend of cell growth was also supported by the evolution of cell area coverage with culture time on the various surfaces (Figure 3C). Much higher cell area coverage on the 0.25 – 2.0PDAs was observed than 4.0PDA as well as TiO_2. It is also worth noting that HUVECs became fully confluent on the 0.25 – 2.0PDAs, but not on either 4.0 PDA or TiO_2 after 72 h culturing (Figure 3A).

In addition, the time-dependent changes of the projected cell area were quite similar among all surfaces: it increased from 2 h to 24 h and sharply decreased at 72 h (Figures 3D). Notably, the projected cell area on all the PDA coatings was much smaller than TiO_2 after 72 h culturing, suggesting better cell division on the PDA coatings. The minor/major axis ratio of HUVECs suggested no apparent difference in the shape of cells on the various PDA coatings after 2 and 24 h culturing, but the cells seemed to be more elongated on the PDA coatings than TiO_2 after 72 h culturing (Figures 3E).

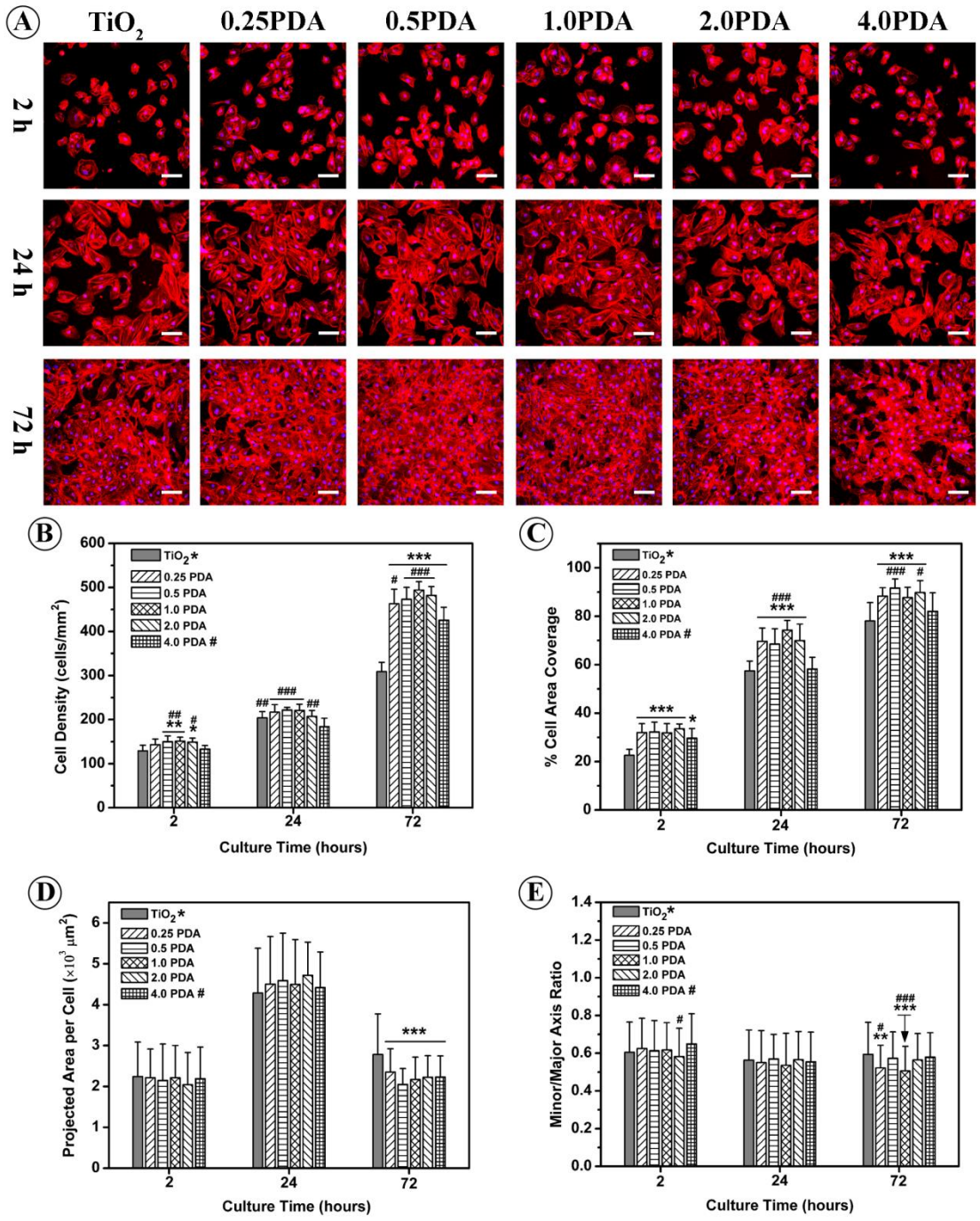

Figure 3. Analysis of EC attachment, proliferation, and morphology on the PDA and TiO_2 surfaces. (A) The morphology of ECs revealed by immunofluorescence staining of cytoskeletal F-actin (red) and nuclei (DAPI, blue). Scale bars: 100 μm. (B) The cell density, (C) area coverage by ECs on various surfaces (D) projected area per cell, and (E) minor/major axis ratio of ECs over time. The cell density and the area coverage

were analyzed from at least 12 images of each surface ($n \geq 12$). The projected area per cell and the minor/major axis ratio were calculated from at least 120 cells from six different images of each surface ($n \geq 120$). Statistically significant differences are marked as follows: * vs. TiO_2; # vs. 4.0PDA.

3.3.2 Focal adhesion studies

Focal adhesions (FAs) serve as cell cytoskeleton-matrix connections and may mediate cell spreading, differentiation, migration and apoptosis [22-24]. As shown in Figure 4A, the PDA coatings induced substantially different FA and stress fiber development compared to TiO_2. Relatively sparse FA with dot shape was induced by TiO_2, and most FAs as well as stress fibers were exclusively distributed around the periphery of the cell on TiO_2. By contrast, all the PDA coatings induced densely distributed FAs all over the cell. The dash-shaped FAs followed the stress fibers to elongate, while the dot-shaped FAs resided at the end of the stress fibers on the PDA coatings. Notably, in contrast to the absence of stress fiber and FA in the perinuclear region on TiO_2, all PDA coatings induced distinguishable bundles of stress fibers and strongly elongated FAs. This substantial difference may suggest disparate distributions of contractility-force profile and levels of mechanosensation in cells induced by the PDA coatings *vs.* TiO_2 [25, 26].

To better quantify the FA development described above, FA number, area fraction, size, and aspect ratio were determined. The PDA coatings induced substantially more FAs formation and increased FA number by 1-fold compared to TiO_2 (Figures 4B and

4C). The FA size was significantly smaller on the PDA coatings than on TiO_2 (Figure 4D). Meanwhile, relatively higher FA aspect ratio, i.e. more elongated FA, was induced by the PDA coatings compared to that on TiO_2 (Figure 4E). The observations indicated that the PDA coatings affected focal adhesion signaling pathway in HUVECs and therefore modulated cell attachment and growth.

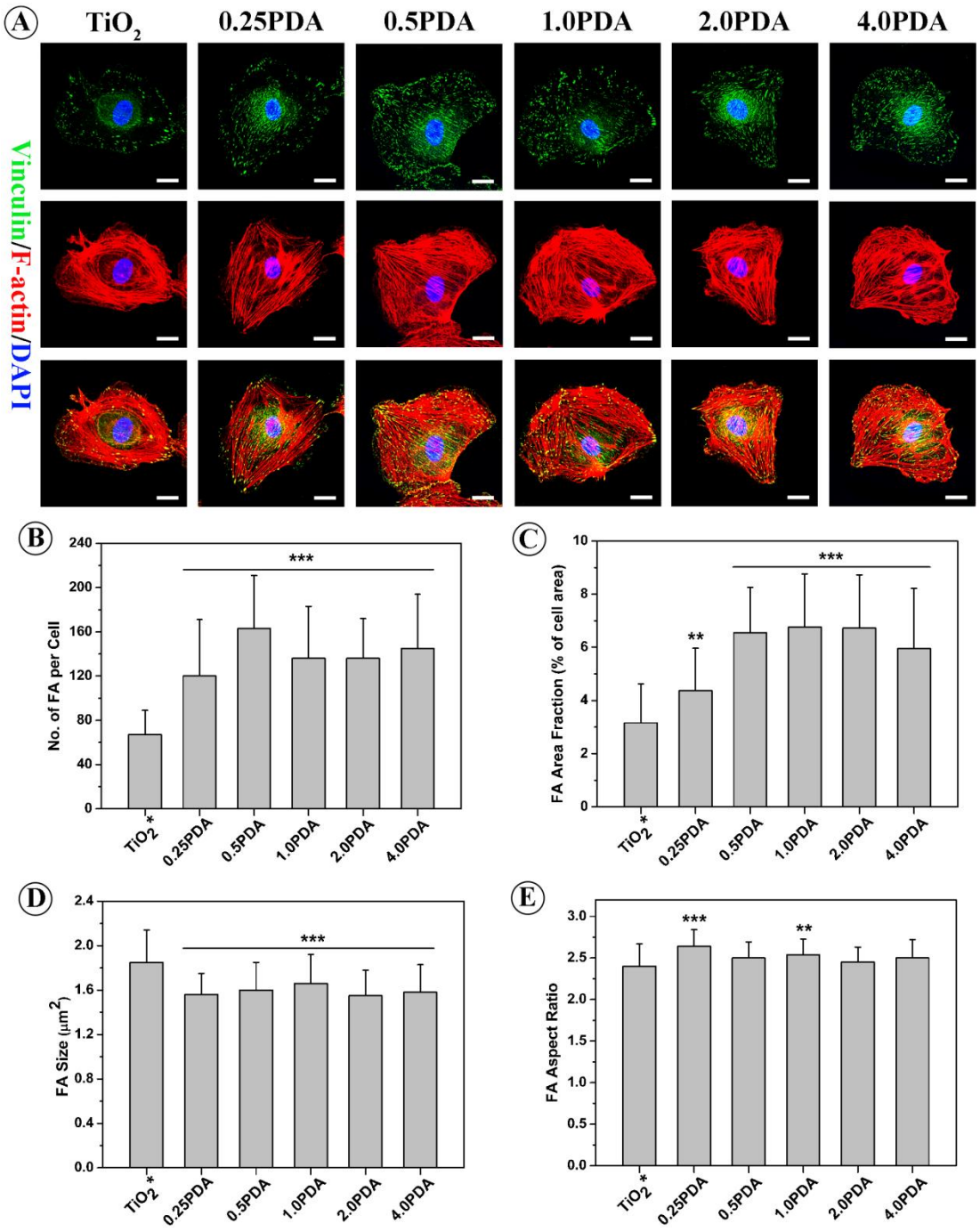

Figure 4. Effects of the PDA coatings on focal adhesion (FA) and stress fiber development. (A) Fluorescent images showing distinct development of vinculin (green) and F-actin (red) as well as nuclei (DAPI, blue) in cells on various surfaces. Scale bars: 20 μm. (B) Number of FA per cell, (C) FA area fraction, (D) FA size, and (E) FA aspect ratio in cells on the various surfaces, which were analyzed from at least 50 cells on each surface ($n \geq 50$). Statistically significant differences are marked as follows: * vs. TiO_2.

3.3.3 Cell phenotype

As shown in Figure 5A, CD31 was restricted to the perinuclear region of cells cultured on TiO_2. By contrast, CD31 was concentrated at the whole intercellular junctions of the cells cultured on the PDA coatings. The relative expression of CD31 on the various surfaces was quantified (Figure 5B): a significantly higher CD31 expression was observed on the 0.25 – 2.0PDA compared to that on TiO_2 as well as on 4.0PDA. These observations suggested the cells cultured on the PDA coatings interacted well with each other and formed stable cell-cell contacts. In addition, a punctate labeling of vWF was clearly detected within the cytoplasm of HUVECs cultured on the various surfaces. However, the relative expression of vWF seemed not to be significantly affected by the PDA coatings (Figure 5C).

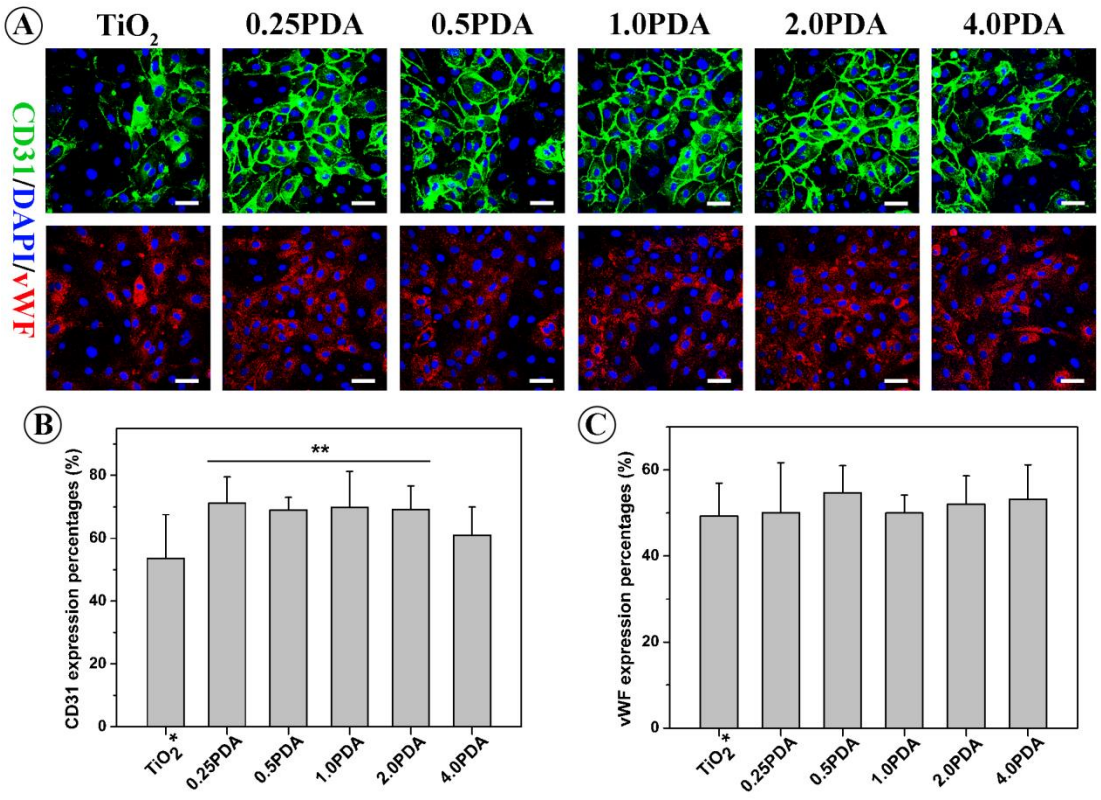

Figure 5. Effects of the PDA coatings on EC phenotype. (A) Fluorescent images showing different development of CD31 (green) and vWF (red) as well as nuclei (DAPI, blue) in cells on the various surfaces. Scale bars: 50 μm. Quantitation of relative expression of (B) CD31 and (C) vWF (cells with positive CD31 or vWF staining / total cell number; $n \geq 12$). Statistically significant differences are marked as follows: * vs. TiO_2.

3.4 HUASMC growth

The growth of HUASMCs was suppressed by the PDA coatings (Figure 6A). After culturing for 24 h, much fewer cells were observed on the PDA coatings, especially on 0.5PDA and 1.0PDA, than that on TiO_2. After culturing for 72 h, the TiO_2 surface induced a typical hill-and-valley growth pattern of cells, as well as 0.25PDA, 2.0PDA,

and 4.0PDA. By contrast, the cells cultured on 0.5PDA and 1.0PDA were more isolated.

Further quantification of HUASMC proliferation showed that the PDA coatings suppressed cell proliferation in a concentration dependent manner with respect to TiO_2 (Figure 6B). After 24 h culturing, 0.5PDA, 1.0PDA, and 2.0PDA induced much lower levels of cell proliferation than TiO_2, whereas the inhibitory effects induced by 0.25PDA and 4.0PDA were not significant. Similar suppression in cell proliferation was observed after 72 h culturing, but only 1.0PDA showed significant inhibitory effect. These results suggested that the PDA coating did inhibit HUASMC proliferation in a dopamine concentration dependent manner.

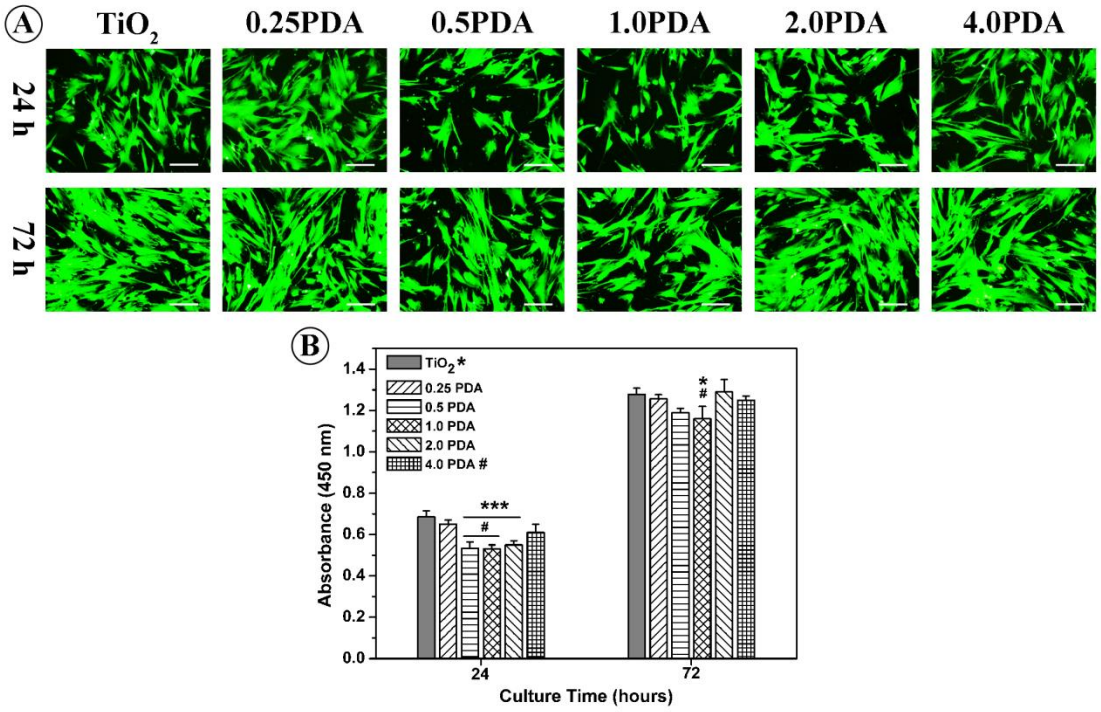

Figure 6. Effects of the PDA coatings on SMC growth after culturing for 24 h and 72 h. (A) Fluorescent images showing α-SMA of SMCs on the various surfaces. Scale

bars: 100 μm. (B) SMC proliferation on the various surfaces. Statistically significant differences are marked as follows: * vs. TiO_2; # vs. 4.0PDA.

3.5 Platelet adhesion

The PDA coatings induced much higher levels of platelet adhesion, but did not significantly influence platelet activation (Figure 7). The number of platelets on all the PDA coatings was significantly higher than TiO_2 (Figure 7B). Notably, 2.0PDA showed the highest number of platelets, while 4.0PDA showed the lowest number of platelets among the various PDA coatings. Most platelets that adhered on the PDA coatings displayed dendritic morphology suggesting non-activated states, which was similar to platelet morphology on TiO_2.

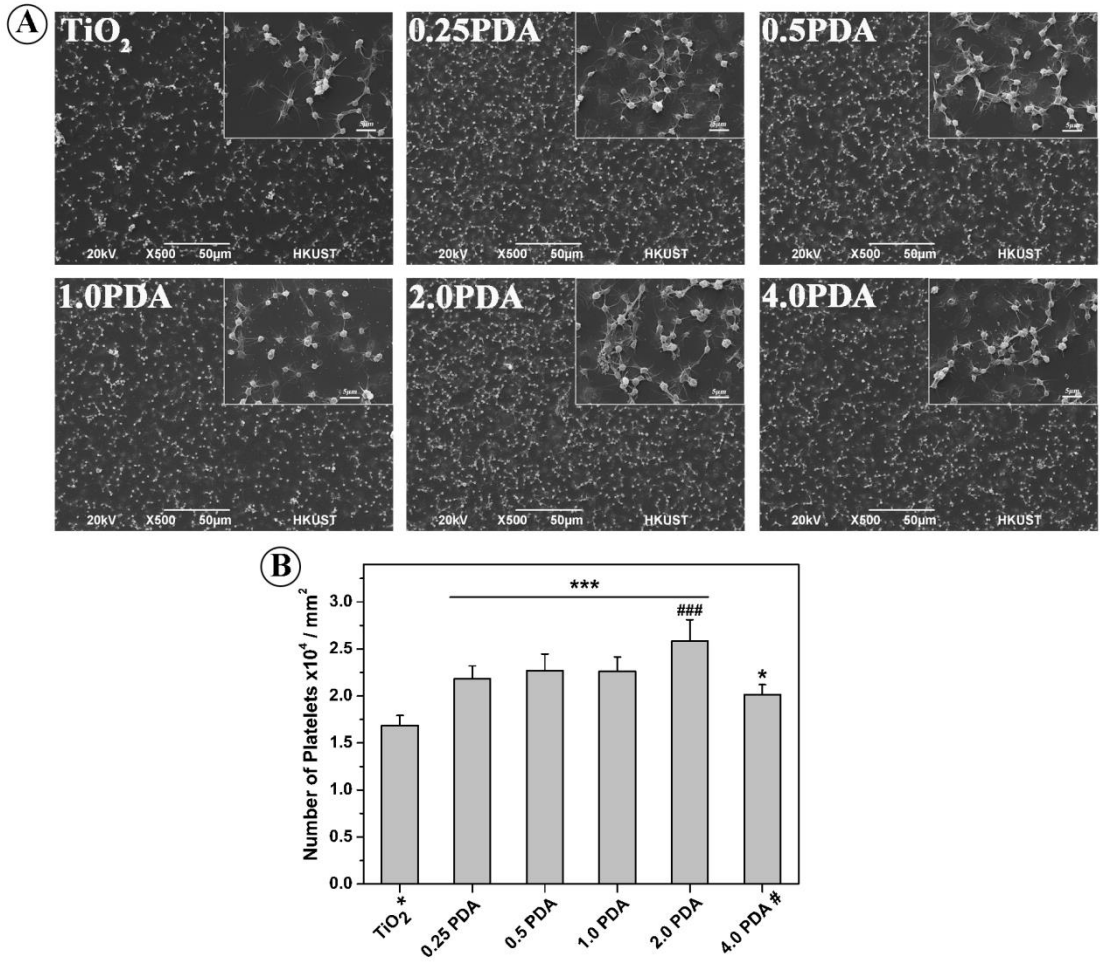

Figure 7. Effects of the PDA coatings on platelet adhesion. (A) SEM images of adherent platelets on the various surfaces after culturing for 2 h in PRP. (B) Quantitative analysis of number of adherent platelets on the various surfaces, which were analyzed from at least five random SEM images at 500 × magnification ($n \geq 5$). Statistically significant differences are marked as follows: * vs. TiO_2; # vs. 4.0PDA.

4. Discussions

The PDA coating induced much higher levels of protein adsorption, enhanced EC growth, inhibited SMC proliferation, and increased platelet adhesion with respect to the pristine TiO_2 surface. Moreover, we found varying synthetic conditions of the

PDA coating indeed resulted in different physicochemical properties, especially the reactive phenolic hydroxyl groups, and different inhibitory effects on SMC proliferation. To explore the mechanism of PDA modulating vascular cell behavior, we analyzed correlations of "surface property – protein adsorption – vascular cell behavior" as summarized in Figure 8.

The experimental results showed that all the PDA coatings displayed much higher levels of adsorption of BSA, Fg, Fn and total serum protein than the TiO_2 surface. It has been reported that the adsorbed protein layer is affected by surface properties such as wettability [27], surface charge [28], topography [29], and chemical functionality [30]. In the present study, lack of substantial differences in water contact angles (~56 – 70^o) and zeta potentials (~-15 – -17eV) among all the surfaces suggest that surface wettability and surface charge are not solely predictive of the protein adsorption characteristics of a substrate. Note that the PDA coating with quinone groups was capable of conjugating with biomolecules containing thiols or primary amines visa imine formation and/or Michael addition [31], the covalent conjugation might account for higher levels of protein adsorption to the PDA coatings as compared to TiO_2. In line with this notion, the higher adsorption levels of BSA and Fg on the 0.25PDA could be, at least partially, ascribed to higher content of quinone with respect to other PDA coatings (data not shown).

We observed that the DPA coating induced a faster and better response of HUVECs. Tsai et al. suggested that the enhancement of cell adhesion to PDA coating could be due to increased immobilization of adhesive proteins such as Fn on the

substrate [4]. Cell adhesion on the substrates can be triggered by binding between adhesion receptors such as integrin on the cell surface and extracellular ligands such as Fn adsorbed on the substrates [32]. Binding of integrin with integrin ligands not only promotes cell adhesion [33-35], but also activates FA signaling pathway, which can increase formation of FAs, regulate actin cytoskeleton organization, and then promote cell spreading and growth [36, 37]. Consistent with this notion, we found that the PDA coatings bound a higher amount of adhesive protein Fn than TiO_2. Moreover, the PDA coatings with higher adsorption levels of Fn not only increased EC attachment number, but also significantly enhanced formation of FAs and stress fibers. Therefore, the increased Fn adsorption resulting from quinone groups on the PDA coatings should be mainly responsible for enhanced EC attachment, favorable FA development and actin cytoskeleton organization. However, it is worth noting that the 2.0PDA displayed substantially higher levels of EC attachment and growth than TiO_2 although a similar amount of Fn adsorption was obtained on these two surfaces, which may be due to the better preserved bioactivity of Fn adsorbed to the PDA coating [3]. Nevertheless, further study on protein conformation is needed to better understand this observation.

In contrast to favorable HUVEC responses, the PDA coating inhibited SMC growth. The biphasic inhibition of SMC growth was induced by the various PDA coatings and was maximized on 1.0PDA, which correlated well with the amount of reactive phenolic hydroxyl groups (Figure 1D). Several studies have indicated that natural polyphenols, like Epigallocatechin-3-*O*-gallate (EGCG), inhibit proliferation

and migration of both smooth muscle cells and endothelial cells [38-41]. Meanwhile, some reports disputed that by finding polyphenols showed much less cytotoxicity against endothelial cells [42], and the inhibition of EC was found to occur at a much higher dose of EGCG as compared to SMC [41]. Although the mechanisms responsible for inhibitory effects of polyphenols on SMC have not been clearly elucidated, a number of reports have shown that these inhibitory effects could be closely related to antioxidant properties of polyphenols [41, 43]. These previous studies strongly support the good correlation found in the present study between inhibitory effect of the PDA coating on SMC and the presence of reactive phenolic hydroxyl groups, which render antioxidant properties to the PDA coating.

In summary, we reason that vascular cell behavior on the PDA coating is governed by its distinctive surface functionality, i.e. the quinone and reactive phenolic hydroxyl groups. On one hand, the presence of quinone groups on the PDA coating induces substantially higher levels of adhesive protein Fn, in turn triggering favorable vascular cell attachment, FA development, stress fiber formation, and cell growth. On the other hand, the presence of reactive phenolic hydroxyl groups on the PDA coating tends to inhibit vascular cell growth, and such inhibitory effect on SMC was much stronger than that on EC.

Herein, we propose that adhesive protein adsorption and subsequent activation of integrin-mediated FA signaling pathway dominate EC response. The inhibitory effects induced by reactive phenolic hydroxyl groups override the effects of adhesive protein adsorption in modulating SMC response. Therefore, the combination of these two

competitive effects endow the vascular cell selectively of the PDA coating, i.e. promoting EC attachment and growth, while inhibiting SMC growth. Notably, the extent of vascular cell selectively was biphasically dependent on initial dopamine concentrations and maximized at the concentration of 1.0 g/L. This is a promising result and could potentially be applied to the design of vascular stents to address the issues associated with re-endothelialization and restenosis.

Apart from vascular cell selectivity, the experimental results indicate that the PDA coating increased platelet adhesion. It is believed that non-adhesive protein such as albumin adsorption would lead to passivation of a surface thereby decreasing cell and platelet attachment [44]. However, the ability of a substrate to inhibit platelet adhesion does not appear to be improved by the adsorption of albumin as evidenced by the increased platelet adhesion on the PDA coatings, which is consistent with other studies of platelet adhesion [45-47]. Note that adsorbed Fg is involved in blood clotting and platelet adhesion by serving as a ligand for the $\alpha_{IIb}\beta_3$ integrin receptor on the platelet membrane [13, 48]. Therefore, much higher Fg adsorption to the PDA coating seems to take a dominant role in increasing platelet adhesion.

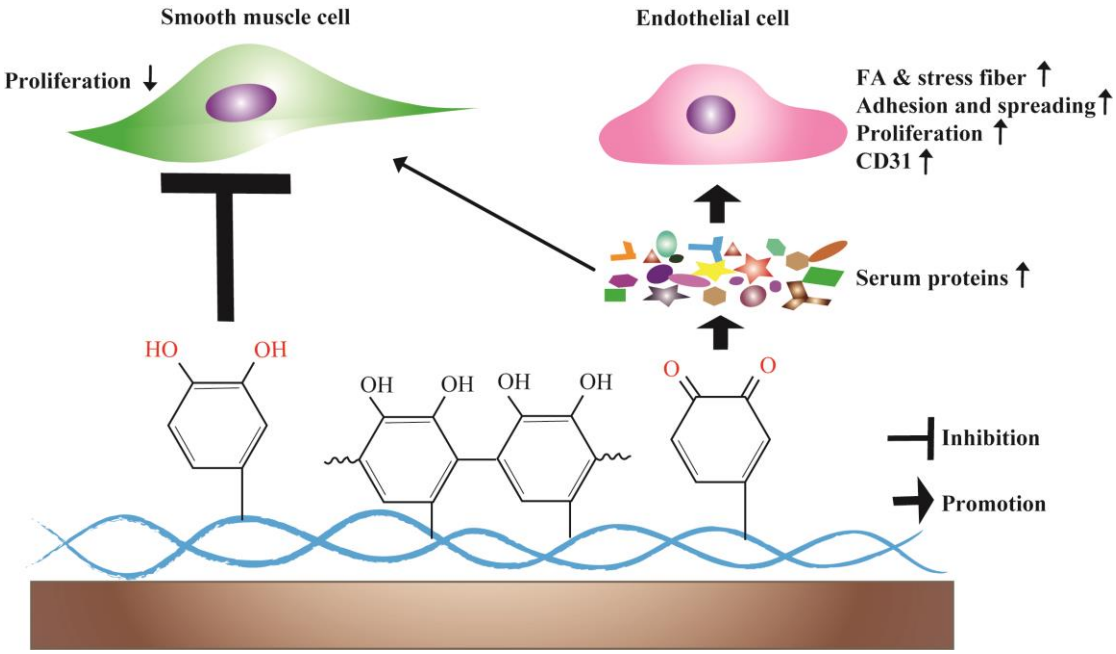

Figure 8. Schematic diagram for proposed mechanism of PDA selectively modulating endothelial cell and smooth muscle cell behavior.

5. Conclusions

Experimental results demonstrate that mussel-inspired surface functionalization of the PDA coating not only influences protein adsorption, but also substantially modulates cellular fates of ECs, SMCs and platelets. The results indicate that the quinone group presented on the PDA coating enhances adsorption of adhesive proteins such as Fn that plays a key role in promoting cell attachment, FA development, stress fiber formation and cell growth of ECs. However, the reactive phenolic hydroxyl group presented on the PDA coating is mainly responsible for inhibiting SMC growth. In addition, the study implicates the importance of initial dopamine concentrations for synthesizing the PDA coating. The PDA coating synthesized at initial dopamine concentration of 1.0 g/L displays the most favorable vascular cell selectivity,

considering as an optimized synthetic condition of the PDA coating in the surface modification of vascular stents.

Acknowledgements

The authors wish to thank Dr. Lutao Weng for his advice and discussion. This work was financially supported by the Research Grants Council of Hong Kong (FSGRF13EG58), Program for New Century Excellent Talents in University (NCET-10-0704), and Sichuan Youth Science Technology Foundation (2011JQ0010).

References

1. S. H. Ku and C. B. Park, *Advanced Healthcare Materials*, 2013, **2**, 1445-1450.
2. S. H. Ku and C. B. Park, *Biomaterials*, 2010, **31**, 9431-9437.
3. S. H. Ku, J. Ryu, S. K. Hong, H. Lee and C. B. Park, *Biomaterials*, 2010, **31**, 2535-2541.
4. W. B. Tsai, W. T. Chen, H. W. Chien, W. H. Kuo and M. J. Wang, *Acta Biomaterialia*, 2011, **7**, 4187-4194.
5. Z. Yang, Q. Tu, Y. Zhu, R. Luo, X. Li, Y. Xie, M. F. Maitz, J. Wang and N. Huang, *Advanced Healthcare Materials*, 2012, **1**, 548-559.
6. R. Luo, L. Tang, S. Zhong, Z. Yang, J. Wang, Y. Weng, Q. Tu, C. Jiang and N. Huang, *ACS Applied Materials and Interfaces*, 2013, **5**, 1704-1714.
7. C. Wu, W. Fan, J. Chang and Y. Xiao, *Journal of Materials Chemistry*, 2011, **21**, 18300-18307.

8. M. Xu, Y. Zhang, D. Zhai, J. Chang and C. Wu, *Biomaterials Science*, 2013, **1**, 933-941.

9. C. Wu, P. Han, X. Liu, M. Xu, T. Tian, J. Chang and Y. Xiao, *Acta Biomaterialia*, 2014, **10**, 428-438.

10. M. Rabe, D. Verdes and S. Seeger, *Advances in Colloid and Interface Science*, 2011, **162**, 87-106.

11. J. L. Brash, *Journal of Biomaterials Science, Polymer Edition*, 2000, **11**, 1135-1146.

12. D. J. Iuliano, S. S. Saavedra and G. A. Truskey, *Journal of Biomedical Materials Research*, 1993, **27**, 1103-1113.

13. M. S. Lord, B. Cheng, S. J. McCarthy, M. Jung and J. M. Whitelock, *Biomaterials*, 2011, **32**, 6655-6662.

14. F. Bernsmann, A. Ponche, C. Ringwald, J. Hemmerle, J. Raya, B. Bechinger, J. C. Voegel, P. Schaaf and V. Ball, *Journal of Physical Chemistry C*, 2009, **113**, 8234-8242.

15. J. Jiang, L. Zhu, B. Zhu and Y. Xu, *Langmuir*, 2011, **27**, 14180-14187.

16. V. Ball, D. D. Frari, V. Toniazzo and D. Ruch, *Journal of Colloid and Interface Science*, 2012, **386**, 366-372.

17. Y. M. Shin, Y. B. Lee and H. Shin, *Colloids and Surfaces B: Biointerfaces*, 2011, **87**, 79-87.

18. Y. Ding, Y. Leng, N. Huang, P. Yang, X. Lu, X. Ge, F. Ren, K. Wang, L. Lei and X. Guo, *Journal of Biomedical Materials Research - Part A*, 2012.

19. T. L. Slocum and J. D. Deupree, *Analytical Biochemistry*, 1991, **195**, 14-17.

20. G. Sauerbrey, *Zeitschrift für Physik*, 1959, **155**, 206-222.

21. C. A. Rice-Evans, N. J. Miller and G. Paganga, *Free Radical Biology and Medicine*, 1996, **20**, 933-956.

22. J. T. Parsons, A. R. Horwitz and M. A. Schwartz, *Nature Reviews Molecular Cell Biology*, 2010, **11**, 633-643.

23. H. Yu, Y. S. Lui, S. Xiong, W. S. Leong, F. Wen, H. Nurkahfianto, S. Rana, D. T. Leong, K. W. Ng and L. P. Tan, *Stem Cells and Development*, 2013, **22**, 136-147.

24. D. H. Kim and D. Wirtz, *FASEB Journal*, 2013, **27**, 1351-1361.

25. A. Besser and S. A. Safran, *Biophysical Journal*, 2006, **90**, 3469-3484.

26. D. H. Kim, A. B. Chambliss and D. Wirtz, *Soft Matter*, 2013, **9**, 5516-5523.

27. J. H. Lee and H. B. Lee, *Journal of biomaterials science. Polymer edition*, 1993, **4**, 467-481.

28. Y. X. Ding, S. Streitmatter, B. E. Wright and V. Hlady, *Langmuir*, 2010, **26**, 12140-12146.

29. M. S. Lord, M. Foss and F. Besenbacher, *Nano Today*, 2010, **5**, 66-78.

30. Y. Arima and H. Iwata, *Biomaterials*, 2007, **28**, 3074-3082.

31. H. Lee, J. Rho and P. B. Messersmith, *Advanced Materials*, 2009, **21**, 431-434.

32. M. C. Siebers, P. J. Ter Brugge, X. F. Walboomers and J. A. Jansen, *Biomaterials*, 2005, **26**, 137-146.

33. J. Wei, T. Igarashi, N. Okumori, T. Maetani, B. Liu and M. Yoshinari,

Biomedical Materials, 2009, **4**.

34. A. L. Koenig, V. Gambillara and D. W. Grainger, *Journal of Biomedical Materials Research - Part A*, 2003, **64**, 20-37.

35. L. T. Allen, M. Tosetto, I. S. Miller, D. P. O'Connor, S. C. Penney, I. Lynch, A. K. Keenan, S. R. Pennington, K. A. Dawson and W. M. Gallagher, *Biomaterials*, 2006, **27**, 3096-3108.

36. N. O. Carragher and M. C. Frame, *Trends in Cell Biology*, 2004, **14**, 241-249.

37. X. Chen, Y. D. Su, V. Ajeti, S. J. Chen and P. J. Campagnola, *Cellular and Molecular Bioengineering*, 2012, **5**, 307-319.

38. H. G. Yoo, B. A. Shin, J. C. Park, H. S. Kim, W. J. Kim, K. O. Chay, B. W. Ahn, R. K. Park, L. M. Ellis and Y. D. Jung, *Anticancer Research*, 2002, **22**, 3373-3378.

39. T. Kondo, T. Ohta, K. Igura, Y. Hara and K. Kaji, *Cancer Letters*, 2002, **180**, 139-144.

40. Z. Y. Chen, W. I. Law, X. Q. Yao, C. W. Lau, K. Ho Water Kwok and Y. Huang, *Acta Pharmacologica Sinica*, 2000, **21**, 835-840.

41. D. W. Han, D. Y. Jung, J. C. Park, H. H. Cho, S. H. Hyon and D. K. Han, *Journal of Biomedical Materials Research - Part A*, 2010, **95 A**, 424-433.

42. M. Inoue, R. Suzuki, N. Sakaguchi, Z. Li, T. Takeda, Y. Ogihara, J. Bao Yuan and Y. Chen, *Biological and Pharmaceutical Bulletin*, 1995, **18**, 1526-1530.

43. R. Locher, L. Emmanuele, P. M. Suter, W. Vetter and M. Barton, *European Journal of Pharmacology*, 2002, **434**, 1-7.

44. R. A. Smith, M. W. Mosesson, A. U. Daniels and T. K. Gartner, *Journal of Materials Science: Materials in Medicine*, 2000, **11**, 279-285.

45. C. D. Tidwell, S. I. Ertel, B. D. Ratner, B. J. Tarasevich, S. Atre and D. L. Allara, *Langmuir*, 1997, **13**, 3404-3413.

46. S. I. Ertel, B. D. Ratner and T. A. Horbett, *Journal of Colloid and Interface Science*, 1991, **147**, 433-442.

47. B. Sivaraman and R. A. Latour, *Biomaterials*, 2009, **31**, 1036-1044.

48. P. Roach, D. Farrar and C. C. Perry, *Journal of the American Chemical Society*, 2005, **127**, 8168-8173.

Graphical Abstract

The relationship of "surface property – protein adsorption – cell behavior" of polydopamine was investigated and the mechanism of polydopamine selectively modulating vascular cell behavior were explored.